Journal of Alloys and Compounds 515 (2012) 171–179

Contents lists available at SciVerse ScienceDirect

Journal of Alloys and Compounds

journal homepage: www.elsevier.com/locate/jallcom

Variations of structure and magnetic properties in UTGe hydrides (T = late transition metal)

A.M. Adamska[a,b,*], L. Havela[a], Y. Skourski[c], A.V. Andreev[d]

[a] Department of Condensed Matter Physics, Faculty of Mathematics and Physics, Charles University, Ke Karlovu 5, 12116 Prague 2, Czech Republic
[b] Faculty of Physics and Applied Computer Science, AGH University of Science and Technology, al. Mickiewicza 30, PL-30 059 Kraków, Poland
[c] Dresden High Magnetic Field Laboratory, Helmholtz-Zentrum Dresden-Rossendorf, 01314 Dresden, Germany
[d] Institute of Physics, Academy of Sciences, Na Slovance 2, 18221 Prague, Czech Republic

ARTICLE INFO

Article history:
Received 13 October 2011
Received in revised form
24 November 2011
Accepted 26 November 2011
Available online 6 December 2011

Keywords:
Actinide alloys and compounds
Metal hydrides
Crystal structure
Magnetization
Magnetic measurements
High magnetic fields

ABSTRACT

Hydrogenation of UTGe compounds results in formation of stable α- and β-hydrides, and modification of the crystal structure and magnetic properties. T_C (3 K) of UCoGe increases up to 50 K in β-hydrides and T_C (9.5 K) of URhGe up to 17 K in α-hydrides. The type of magnetic order is changed in UNiGe-H and UIrGe-H. The observed effects are attributed to the increased U–U spacing in the hydrides.

1. Introduction

Magnetic properties of uranium-based intermetallics are intimately related to the character of the 5*f* electronic states, ranging between a localized character, similar to lanthanides, and itinerancy, which is reminiscent of magnetism emerging in transition metals. For purely band systems, the actinide–actinide spacing is a crucial parameter, which determines the magnetic properties. However, for uranium compounds with the U–U spacing (d_{U-U}) large enough the principal controlling parameter is the 5*f*-ligand hybridization.

Hydrogenation in general leads to changes/modifications of both crystal and electronic structure of intermetallic compounds. It brings a relatively small perturbation to the system, namely a lattice expansion and the hydrogen bonding with other atoms in the lattice. New formed hydrides represent autonomous compounds, often exhibiting new and very interesting physical properties. Besides, studies of their properties can provide additional information on the specific features of interatomic interactions in the initial compounds. Hydrogen absorption in actinide compounds strongly supports the tendency to form local 5*f* magnetic moments and gives rise to magnetic order. This can be partially attributed to 5*f*-band narrowing due to enhanced inter-actinide spacing.

This type of development has already been indicated for selected members of UTX (T = transition metal, X = *p*-element) family. Hexagonal structure (ZrNiAl-type) of UNiAl-H [1], UCoSn-H and URuSn-H [2,3] significantly expands, even up to 12.4% for $UNiAlH_{2.0-2.3}$. The antiferromagnetic (AF) ordering of UNiAl ($T_N = 19$ K) is lost in $UNiAlH_{0.06-0.58}$, changed into ferromagnetic (F) one in $UNiAlH_{0.7}$ ($T_C = 87$ K), and then turns back to AF in $UNiAlH_{2.0-2.3}$ (with higher T_N of 94–117 K). Hydrogen absorption in UCoSn and URuSn causes only the shift of T_C from 82 K up to 102 K in $UCoSnH_{1.4}$ and from 54 K weakly down to 51 K in $URuSnH_{1.4}$. In the case of silicides, such as UCoSi-H, UPdSi-H, UNiSi-H [4,5], the orthorhombic crystal structure (TiNiSi-type) transforms into the hexagonal one (ZrBeSi-type) and expands even by about 8% in $UNiSiH_{1.0}$. The latter is a ferromagnet with $T_C \approx 98$ K, whereas UNiSi is an antiferromagnet with $T_N \approx 85$ K. T_N (≈ 31 K) of UPdSi increases up to 46 K in $UPdSiH_{1.0}$. The volume expansion is not sufficient to induce a magnetic order in UCoSi-H. Other UTSi

---

[*] Corresponding author at: Department of Condensed Matter Physics, Faculty of Mathematics and Physics, Charles University, Ke Karlovu 5, 12116 Prague 2, Czech Republic.

E-mail address: anna@mag.mff.cuni.cz (A.M. Adamska).

0925-8388/$ – see front matter © 2011 Elsevier B.V. All rights reserved.
doi:10.1016/j.jallcom.2011.11.131

compounds did not exhibit any noticeable H absorption. Replacing Si by larger Ge provides larger interstitials, and the hydrogenation conditions may be more favorable due to purely geometrical conditions as the expanded interstitials can allocate hydrogen atoms more easily.

This work presents results of studies of the U magnetism tuned by hydrogen absorption and concomitant lattice expansion in UTGe compounds (stoichiometry 1:1:1), in our case involving T from the end of the 3*d*- (Fe, Co, Ni), 4*d*- (Rh, Pd) and 5*d*- (Ir, Pt) series. In this kind of compounds, the hybridization between the 5*f* and *d*-states is gradually reduced with increasing population of the transition metal *d*-electron states. UTGe compounds crystallize mainly in the orthorhombic TiNiSi-type of structure (an exception is UFeGe, which undergoes a structural phase transition at $T = 500$ K, with the room temperature (RT) phase being monoclinically distorted) [6]. These compounds show, depending mostly on the strength of the 5*f*-ligand hybridization, diverse types of ground state, from Pauli paramagnetism (P) to AF and/or F order. The extremely strong magnetocrystalline anisotropy, with the *a* direction as the general hard anisotropy direction [7] can be related to the *a*-axis alignment of the U chains, whereas the shortest d_{U-U} between the chains is larger than the value within the chain.

Knowing the effects of hydrogen absorption in selected UTX compounds and the structural and magnetic properties of UTGe compounds, it is interesting to investigate hydrogen-induced changes in this particular group of compounds.

2. Experimental details

2.1. Sample preparation

Polycrystalline samples of UTGe (T = Fe, Co, Ni, Rh, Pd, Ir and Pt) were prepared by arc melting of stoichiometric amounts of the constituent metals in a mono-arc furnace under protection of an Ar atmosphere. A heat treatment was only necessary for UCoGe in order to improve the quality of the sample. The as-cast pieces were wrapped in Ta foil and annealed in quartz tubes under a high vacuum, for 24 h at 1200 °C and 20 days at 950 °C. The phase composition was checked by means of XRD-3003 Seifert or Bruker D8 Advance diffractometers with Cu-K$_\alpha$ radiation in a step regime (step of 0.02° for 2θ). The Rietveld analysis of the X-ray diffraction (XRD) data was performed using the FullProf program.

2.2. Hydrogenation and decomposition

The bulk materials were crushed into submillimeter particles and loaded in a reactor for hydrogenation. After so-called activation of the surface by the thermal cycling of sample up to $T = 523$ K in a dynamic vacuum ($p \approx 2 \times 10^{-6}$ mbar), pure hydrogen gas was introduced into the reactor. Depending on its pressure ($p_{H_2} = 0.5$–156 bar), various H stoichiometries could be achieved. Last step of hydrogenation process was the thermal cycling (twice) of the sample up to $T = 773$ K under the given H_2 pressure in order to promote the hydrogen absorption. The crystal structures of the synthesized products were checked by XRD.

The absolute amount of absorbed hydrogen in UTGe hydrides was determined by thermally induced desorption (heating of the sample up to $T \approx 773/673$ K in an evacuated calibrated volume). The crystal structures of the decomposed products were checked by XRD.

2.3. Magnetic and specific-heat measurements

Magnetic measurements on fine powders with particles fixed by a glue in random orientation were performed in Quantum Design Physical Properties Measuring System (PPMS) in the temperature range 2–300 K and external magnetic fields up to 9 T. The *ac* susceptibility ($\chi_{ac}(T)$) was measured in zero *dc* field and *ac* field of 1 mT with frequency 80 Hz. The Magnetic Property Measurement System (MPMS) with Superconducting Quantum Interference Device (SQUID) detection system equipped with a 7 T magnet was used is few cases.

The high-field magnetization curves for UNiGe and its β-hydrides were measured at $T = 1.5$ K on random powders fixed by cyanoacrylate glue, in pulsed magnetic fields up to 60 T (pulse duration 20 ms) at High-field Laboratory in Dresden, Germany. The magnetization was measured by the induction method using a coaxial pick-up coil system. Detailed description of high-field installation is given in Ref. [8].

Temperature dependence of specific heat was studied on pellets pressed in a die with tungsten carbide faces also by means of the PPMS system.

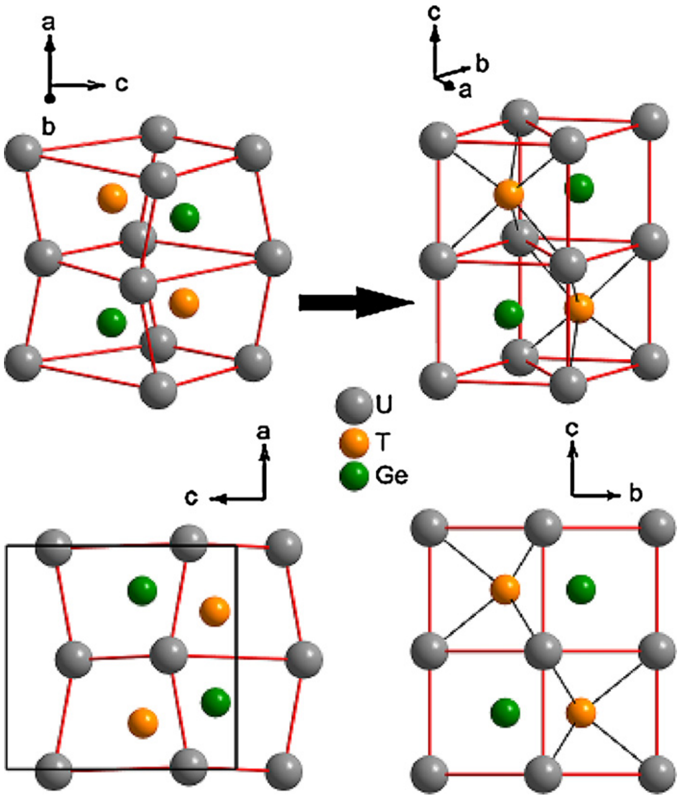

Fig. 1. The relationship between the unit cells of TiNiSi (left) and ZrBeSi (right) structure types and their projections. Hydrogen atoms locate inside the U_3T tetrahedra (max. 2 H/f.u.)..

3. Results and discussion

3.1. Crystal structure

The orthorhombic TiNiSi-type of structure (space group *Pnma*), the most common one reported for UTGe compounds, is built of distorted trigonal prisms U_6 centred either by X or by T atoms (atomic positions U – 4*c* (x_U; 0.25; z_U); T – 4*c* (x_T; 0.25; z_T); X – 4*c* (x_{Ge}; 0.25; z_{Ge})). It is an ordered variant of the $CeCu_2$ structure considered as a distortion of the hexagonal AlB_2 structure.

UTGe compounds were found to absorb hydrogen, forming stable α- or/and β-hydrides. The exception is UPtGe. This compound does not absorb any noticeable amount of hydrogen up to $p_{H_2} = 156$ bar and $T = 773$ K. Lattice parameters of UTGe and their hydrides are presented in Table 1. The label of an α-hydride is used to describe a solid solution of a small amount of hydrogen randomly distributed in the lattice. Such hydride adopts the TiNiSi-type of structure, slightly expanded. A β-hydride is the H-rich phase significantly expanded, adopting in our case the ZrBeSi-type of structure.

The ZrBeSi-type of structure (space group $P6_3/mmc$) is closely related to the TiNiSi-type, which can be also considered as orthorhombically deformed hexagonal ZrBeSi-type of structure (superstructure to AlB_2-type). Due to formal reasons, the crystal axes are interchanged between the hexagonal and orthorhombic structures. The simple relation between the lattice parameters of these two structure types is: $c_{hex} = a_{orth}$ and $a_{hex} = b_{orth} = c_{orth}/\sqrt{3}$. The relationship between the TiNiSi and ZrBeSi structure types is illustrated in Fig. 1.

Based on the rare-earth (R) ternary compound as $LaNiSnD_2$ [9,10] with a similar structure transformation upon hydrogenation as reported for UTSi and UTGe compounds, it was found that

Table 1
Summary of the crystal structure parameters (lattice parameters *a*, *b* and *c*, unit cell volume *V*, relative volume expansion $\Delta V/V$, the shortest d_{U-U}) for UTGe compounds and their hydrides.

Compound	p_{H_2} (bar)	Structure type	a (Å)	b (Å)	c (Å)	V/f.u. (Å^3)	$\Delta V/V$ (%)	d_{U-U} (Å)
UFeGe[c]	–	Monoclinic (β = 93.7°)	6.977(1)	4.305(1)	6.983(1)	52.33	–	3.45
$UFeGeH_{0.3}$[c]	2	TiNiSi (α-hydride)	6.781(2)	4.182(1)	7.412(2)	52.55	0.5	3.45
$UFeGeH_{1.7}$[c]	156	ZrBeSi (β-hydride)	4.176(1)	–	7.337(2)	55.42	6.0	3.67
UCoGe[d]	–	TiNiSi	6.848(1)	4.207(1)	7.230(1)	52.07	–	3.48
$UCoGeH_{0.1}$[d]	0.5	TiNiSi (α-hydride)	6.851(1)	4.201(1)	7.254(1)	52.19	0.23	3.48
$UCoGeH_{1.7}$[a,d]	2	ZrBeSi (β-hydride)	4.095(1)	–	7.937(1)	57.64	10.70	3.97
$UCoGeH_x$[d]	135	ZrBeSi						
		β (63%)	4.098(1)	–	7.907(3)	57.49	10.40	3.95
		β' (36%)	4.114(3)	–	7.624(8)	55.86	7.30	3.81
$UCoGeH_x$[d]	140	ZrBeSi						
		β (10%)	4.109(5)	–	7.842(9)	57.16	9.80	3.92
		β' (89%)	4.125(1)	–	7.517(2)	55.38	6.40	3.76
UNiGe[e]	–	TiNiSi	7.000(3)	4.233(2)	7.197(2)	53.31	–	3.56
$UNiGeH_{0.3}$[e]	dec[b]	ZrBeSi (β-hydride)	4.113(1)	–	7.596(2)	55.66	4.4	3.80
$UNiGeH_{1.0}$[e]	2	ZrBeSi (β-hydride)	4.108(1)	–	7.714(2)	56.38	5.8	3.86
$UNiGeH_{1.2}$[e]	156	ZrBeSi (β-hydride)	4.096(1)	–	7.891(3)	57.33	7.6	3.95
URhGe[f]	–	TiNiSi	6.876(2)	4.333(1)	7.507(2)	55.92	–	3.50
$URhGeH_{0.1}$[f]	130	TiNiSi (α-hydride)	6.898(2)	4.318(1)	7.583(3)	56.47	1.0	3.52
$URhGeH_{0.3}$	156	TiNiSi (α-hydride)	6.906(5)	4.316(3)	7.604(5)	56.67	1.3	3.52
UPdGe	–	TiNiSi	7.049(3)	4.354(2)	7.612(3)	58.40	–	3.60
$UPdGeH_{0.1}$	152	TiNiSi (α-hydride)	7.110(3)	4.335(2)	7.618(2)	58.71	0.5	3.63
UIrGe	–	TiNiSi	6.867(1)	4.302(1)	7.576(1)	55.96	–	3.51
$UIrGeH_{0.1}$	148	TiNiSi (α-hydride)	6.880(2)	4.304(1)	7.609(2)	56.33	0.7	3.52

[a] 4% of the phase was recognized as $UCoGeH_{0.1}$.
[b] Partial decomposition of $UNiGeH_{1.0}$.
[c] [12].
[d] [13].
[e] [14].
[f] [15].

one type of D/H positions, surrounded by R_3T in tetrahedral coordination, is occupied. This means that the deuterium atoms in the ZrBeSi-type of structure tend to occupy the $4f$ (1/3, 2/3, z) sites. The theoretical maximal occupation of each trigonal prism with R atoms in the corners and T atoms in the centre (forming two R_3T tetrahedra sharing the vertex – T atom) leads to 2 H/f.u. The shortest interatomic distance between deuterium atoms is then $d_{D-D} \approx 2.78$ Å. A similar position of the deuterium atoms inside the U_3Co tetrahedra was reported for deuterated uranium ternary compounds, e.g. $UCoSnD_{0.6}$ with the ZrNiAl-type of structure ($4h$ (1/3, 2/3, z) site) [11].

3.1.1. UFeGe-H

An α-hydride of UFeGe with H content of 0.3 H/f.u. was successfully synthesized under $p_{H_2} = 2$ bar and thermal cycling only up to $T = 723$ K (in order to avoid the structure transformation). The monoclinic symmetry was lifted to orthorhombic, reaching 0.5% of volume expansion, which is clearly the effect of hydrogen absorption. The shortest d_{U-U} ($\approx$3.45 Å) remains unchanged. The expanded orthorhombic structure is stable at RT. During the hydrogenation process under $p_{H_2} = 96$ bar, 80% of the monoclinic phase was transformed into the hexagonal one, the rest (20%) remained as the high-T phase of UFeGe (TiNiSi-type [6]), respectively. An estimation of the H content gave a value 1.7 H/f.u. on average. Estimated H content in both phases is 0.3 H/f.u.$_{\text{orth}}$ and 2.0 H/f.u.$_{\text{hex}}$. In order to avoid the phase coexistence, the highest available H_2 pressure of 156 bar was applied to synthesize a pure β-hydride of UFeGe. The attempt was successful yielding the β-hydride with the unit cell expanded by about 6.0% and the shortest d_{U-U} increased by about 6.4%. The H content was estimated to be 1.7 H/f.u. For more details see Ref. [12].

3.1.2. UCoGe-H

Applied H_2 pressure of 0.5 bar resulted in formation of pure α-hydride with H content of 0.1 H/f.u., expanded by about 0.23% with respect to the parent compound. The shortest d_{U-U} ($\approx$3.48 Å) remains unaffected. Higher H_2 pressure of 1.2 bar yielded a two-phase mixture of α- and β-hydride, i.e. $UCoGeH_{0.1}$ (12%) and $UCoGeH_{1.6}$ (87%). The mean hydrogen concentration is 1.4 H/f.u. The H_2 pressure of 2 bar was already sufficient to synthesize almost pure β-hydride of UCoGe (95%), i.e. $UCoGeH_{1.7}$, expanded by 10.7%, 4% of the material was attributed to the residual α-hydride ($UCoGeH_{0.1}$). The shortest d_{U-U} increases to 3.97 Å, i.e. by about 14% in such β-phase. Other attempts of hydrogenation of UCoGe under $p_{H_2} = 5$, 135 and 140 bar yielded surprisingly two different β-phases with the mean H concentration 1.6, 1.6, 1.0 H/f.u., respectively. An interesting fact is that the higher was the pressure of H_2 loading, the lower was the fraction of the hydride with higher H concentration (see Table 1). The highest H_2 pressure gave almost pure phase (89%) denoted here as the β'-hydride, which also crystallizes in the ZrBeSi-type of structure. The unit cell of the β'-hydride is expanded by about 6.4%, i.e. less than the β-hydride. The shortest d_{U-U} increases to 3.76 Å, i.e. by about 8% relative to UCoGe. The two different forms of the β-hydride may indicate that a full hydrogenation of the only H site (or hydrogenation of another site not accessible at low-p_{H_2}) leaves a state unstable when the H_2 pressure is released and sample exposed to external atmosphere. The H_2 release may then favor the β'-phase. For more details see Ref. [13].

3.1.3. UNiGe-H

β-Hydrides of UNiGe, namely $UNiGeH_{1.2}$, $UNiGeH_{1.0}$ and $UNiGeH_{0.3}$, synthesized under $p_{H_2} = 156$, 2 bar, and by a controlled decomposition of $UNiGeH_{1.0}$, are expanded by 7.6, 5.8, 4.4%, respectively, relative to UNiGe. An increase of d_{U-U} by about 11, 8.4, and 6.7% has been reported. An attempt to obtain an α-hydride by applying relatively low H_2 pressure of 0.6 bar resulted in mixed-phase material. In this case, 45% of the orthorhombic phase was transformed into the hexagonal one with concomitant lattice expansion of 8.8%. The H content was estimated to be 1.2 H/f.u. No expansion is observed for the orthorhombic phase, thus we can conclude that no α-hydride exists. For more details see Ref. [14].

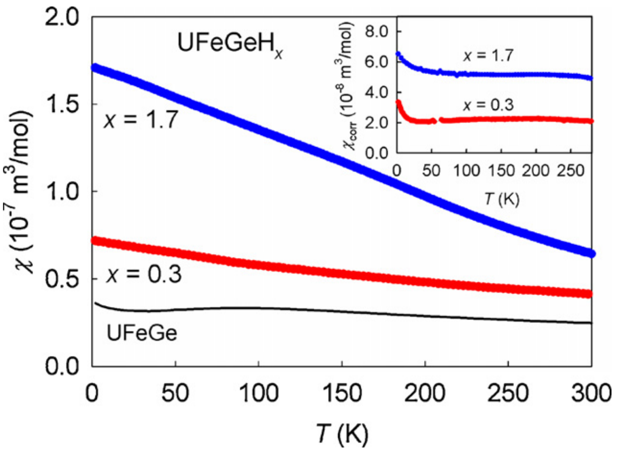

Fig. 2. Temperature dependence of magnetic susceptibilities for UFeGeH$_x$ and UFeGe measured in μ_0H = 2 T [12]. The inset shows the temperature dependence of magnetic susceptibilities corrected for F impurity at T = 300 K.

3.1.4. α-Hydrides of URhGe, UPdGe and UIrGe

Applied H_2 pressure ≥ 130 bar and thermal cycling up to T = 773 K resulted in formation only α-hydrides of URhGe, UPdGe and UIrGe. No β-hydrides were obtained under such conditions. Hydrogen absorption causes a volume expansion of about 1% in URhGeH$_{0.1}$ [15] and 1.3% in URhGeH$_{0.3}$. The shortest d_{U-U} increases by about 0.6% in both of cases. Similar effect of volume expansion is observed in α-hydrides of UPdGe and UIrGe accommodating 0.1 H/f.u. The unit cells of UPdGeH$_{0.1}$ and UIrGeH$_{0.1}$ are expanded by about 0.5 and 0.7%, and the shortest d_{U-U} increase to 3.63 Å and 3.52 Å, i.e. by about 0.8 and 0.3%, respectively.

3.2. Specific heat and magnetic properties

The γ coefficients for selected UTGe hydrides were estimated from the linear extrapolation of C_p/T vs. T^2 to T = 0 K. The fittings (according to the formula: $C_p/T = \gamma + \beta T^2$) were done mostly in the T^2 range between 4 and 200 K^2, yielding the γ coefficients of 36 mJ/mol K^2 for UFeGeH$_{1.7}$ comparing with 12 mJ/mol K^2 for UFeGe [12], 66 mJ/mol K^2 for the α-hydride of UCoGe, 103 mJ/mol K^2 for UCoGeH$_{1.7}$ and 111 mJ/mol K^2 for two-β-phase hydride comparing with 51 mJ/mol K^2 for UCoGe [13], 70 mJ/mol K^2 for UNiGeH$_{1.2}$ in comparison to 23 mJ/mol K^2 for UNiGe [16] and 16 mJ/mol K^2 for UPdGeH$_{0.1}$. An enhancement of γ coefficient by about 200% in UFeGeH$_{1.7}$ and UNiGeH$_{1.2}$ or 100% in UCoGeH$_{1.7}$ means that hydrogenation leads to the 5f-band narrowing and, consequently, to an increase of magnetic moments and/or decrease of the degree of 5f-ligand hybridization. In the case of UFeGe we may speculate that the monoclinic structural distortion is an electronic effect, i.e. derived by the the tendency to shift some electronic states from the Fermi level towards lower energies. In the case of UCoGeH$_{0.1}$ or UPdGeH$_{0.1}$, the γ coefficient slightly increases (by about 30%) or remains almost unchanged, which indicates that hydrogen absorption does not affect much the density of states (DOS) at the Fermi level in these hydrides. The inspection of data in the C_p vs. T representation reveals the Debye temperature Θ_D = 300 K for both above mentioned α-hydrides of UTGe. Simple Debye model does not describe well the $C_p(T)$ for the β-hydrides of UTGe. It may be due to additional entropy related to vibration modes of H in the lattice and possible H diffusion above T = 200 K.

3.2.1. UFeGe-H

Magnetic susceptibilities of UFeGe hydrides increase markedly and become monotonously increasing with decreasing temperature (Fig. 2), exhibiting no phase transition through the whole temperature range measured. The broad maximum (reminiscent of spin fluctuations), reported in UFeGe at 80 K [18], vanishes. Due to a F impurity detected at T = 300 K, magnetic susceptibilities of UFeGe hydrides were corrected yielding a very flat $\chi_{corr}(T)$ on the level of 5×10^{-8} m^3 mol^{-1} for UFeGeH$_{1.7}$ and 2×10^{-8} m^3 mol^{-1} for UFeGeH$_{0.3}$ followed only by a low-T upturns (the inset in Fig. 2). Broad anomalies with maxima between 100 and 150 K for UFeGeH$_{1.7}$ and between 150 and 200 K for UFeGeH$_{0.3}$ detected by ac susceptibility measurements indicate a distribution of F objects with variable T_C in these samples. The magnetization curves of UFeGeH$_{1.7}$ and UFeGeH$_{0.3}$ measured at T = 2 K form hysteresis loops with estimated spontaneous magnetization (μ_s) of ≈0.04 μ_B/f.u. and 0.01 μ_B/f.u., respectively. The relatively high ordering temperatures (or magnetization-freezing temperatures of the "ferromagnetic impurity" clusters) reaching RT suggest a dominant contribution of the Fe-3d magnetism. An increase of d_{U-U} and other types of interatomic spacings is not sufficient to induce a real magnetic order, only the susceptibility increases. The fact that the spontaneous magnetization is not a bulk feature is corroborated by ^{57}Fe Mössbauer spectroscopy. The absence of any magnetic

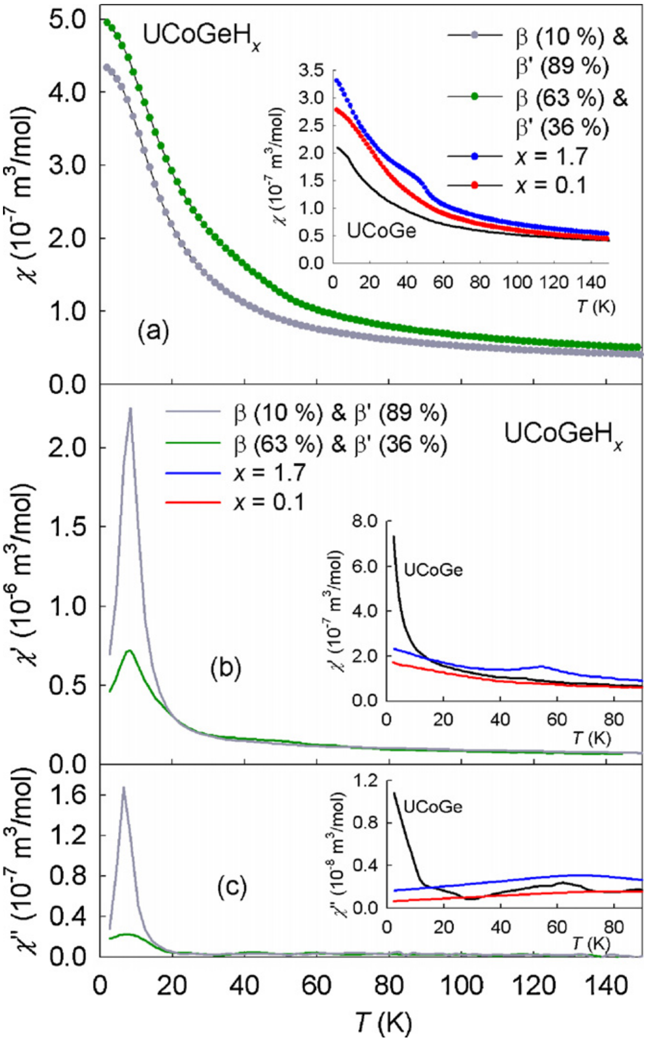

Fig. 3. (a) Temperature dependence of dc susceptibilities for the two-β-phase hydrides of UCoGe, obtained under $p_{H_2} \geq 135$ bar, measured in μ_0H = 2 T [13]. The inset shows $\chi_{dc}(T)$ for almost pure β- and α-hydride of UCoGe compared with the parent compound. (b) Real and (c) imaginary part of ac susceptibilities for high H_2 pressure UCoGeH$_x$. The insets show real and imaginary part of ac susceptibilities for low H_2 pressure UCoGeH$_x$ and UCoGe. $\chi_{ac}(T)$ was measured in zero dc field and ac field of 1 mT and frequency 80 Hz.

ordering down to $T = 0.4$ K for UFeGe and down to $T = 2$ K for its pure β-hydride was established by specific heat measurements. For more details see Ref. [12].

3.2.2. UCoGe-H

The weak F order ($T_C \approx 3$ K) reported in UCoGe [19] is suppressed in the α-hydride. The temperature dependence of *dc* susceptibility ($\chi_{dc}(T)$) for $UCoGeH_{0.1}$ shows no signs of any magnetic transition (Fig. 3(a), the inset). The magnetization curve measured at $T = 2$ K reveals no spontaneous magnetization (the inset in Fig. 4), but its slope is higher than in the parent compound. In the case of almost pure β-hydride, i.e. $UCoGeH_{1.7}$, $\chi_{dc}(T)$ exhibit a F transition in the vicinity of 50 K (the insets in Fig. 3(a) and in Fig. 3(b) and (c)), which is undoubtedly connected with 95% of the hexagonal phase. However, the F state is not complete due to the presence of another phase (paramagnetic α-hydride) in this hydride. The magnetization curve measured at $T = 2$ K shows a part of the hysteresis loop (the inset in Fig. 4). μ_S is not dramatically enhanced, but we can suppose that the F order with 0.05 μ_B/f.u. is intrinsic. In the case of the two-β-phase hydride obtained under $p_{H_2} = 135$ bar, $\chi_{dc}(T)$ shows weakly a F transition below 50 K (Fig. 3(a)). No transition around 50 K is observed for the two-β-phase hydride obtained under $p_{H_2} = 140$ bar. A Ferro transition in the vicinity of 8 K emerges for high H_2 pressure hydrides, and it can be attributed to the β′-phase. A sharp, well pronounced peak around this temperature is seen in $\chi_{ac}(T)$ for the hydride obtained at $p_{H_2} = 140$ bar containing 89% of β′-phase, while for the hydride obtained under $p_{H_2} = 135$ bar containing 36% of β′-phase, the peak is weaker and broader (Fig. 3(b) and (c)). The lack of saturation of *dc* susceptibility for the hydride obtained under $p_{H_2} = 135$ bar, below the first transition at $T_C \approx 50$ K (attributed to β-phase) suggests that this hydride is in fact inhomogeneous. This is due to a fraction of material (β′-phase) with T_C (≈8 K) much lower than 50 K. The magnetization curves measured at $T = 2$ K reveal the part of the hysteresis loop (Fig. 4). μ_s remains in the range 0.05–0.10 μ_B/f.u. The specific heat measurements for UCoGe and its α-hydride (before and after the decomposition) performed down to $T = 0.4$ K, show no anomalies in the whole temperature range. It means that no superconductivity could be observed even in this particular sample of UCoGe, despite long term annealing procedure mentioned in the experimental part. However, the specific heat data display a pronounced anomaly with a maximum at $T = 50$ K for $UCoGeH_{1.7}$. The anomaly is much weaker in the two-β-phase hydride. For more details see Ref. [13].

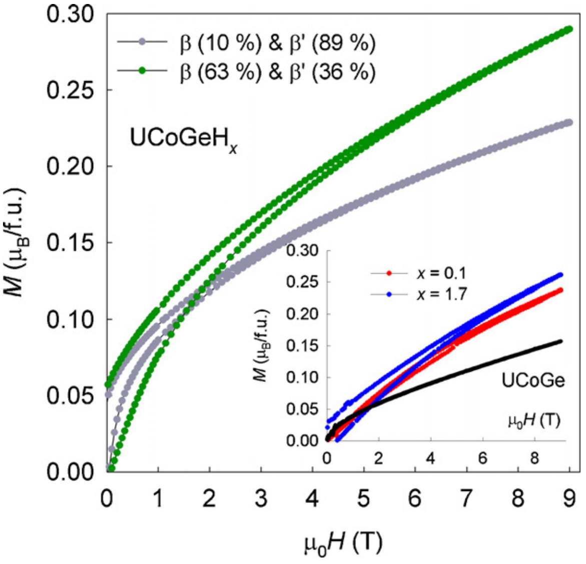

Fig. 4. Comparison of magnetization curves of $UCoGeH_x$ and UCoGe measured at $T = 2$ K [13].

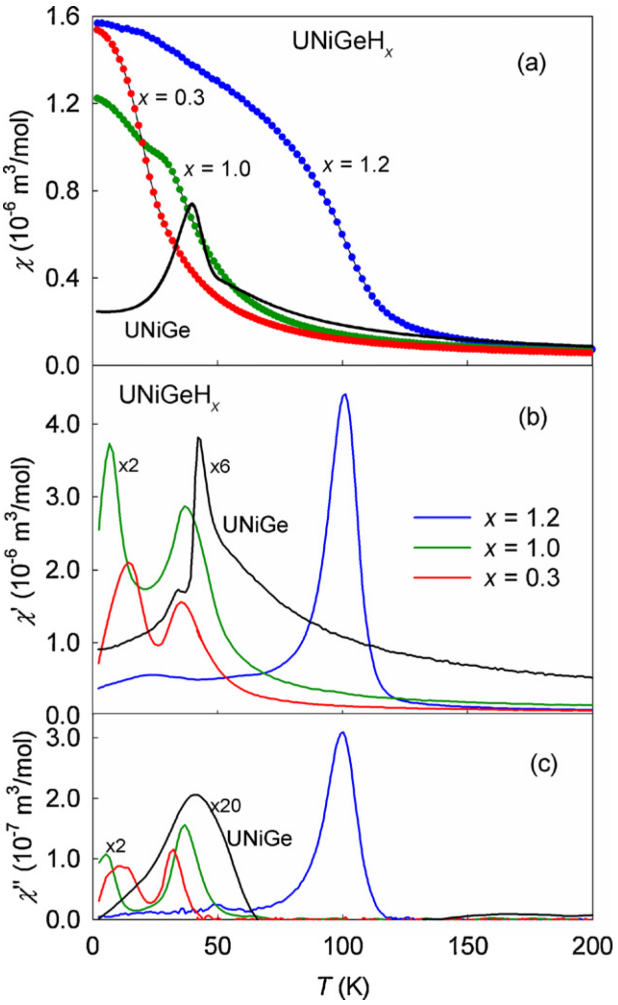

Fig. 5. (a) Temperature dependence of *dc* susceptibilities for $UNiGeH_x$ and UNiGe measured in $\mu_0H = 2$ T [14]. (b) Real and (c) imaginary part of *ac* susceptibilities for $UNiGeH_x$ and UNiGe measured in zero *dc* field and *ac* field of 1 mT and frequency 80 Hz.

3.2.3. UNiGe-H

$\chi_{dc}(T)$ of β-hydride of UNiGe with the highest H concentration i.e. 1.2 H/f.u. exhibits the F-type of behavior (Fig. 5(a)) in contrast to UNiGe (an antiferromagnet below 44 and 50 K [20]). The magnetic transition appears in the vicinity of 100 K (Fig. 5(a)–(c)). Two intermediate hydrides: $UNiGeH_{1.0}$ and $UNiGeH_{0.3}$ exhibit two phase transitions, the first one around $T_N \approx 38$–35 K and the second one at quite low temperatures of 7–15 K. The transitions are better resolved by the *ac* susceptibility study (Fig. 5(b) and (c)). The maxima in $\chi_{ac}(T)$ correspond to respective magnetic ordering temperatures. The magnetization of UNiGe at 60 T reaches approx. 1.6 μ_B/f.u. and has a clearly still increasing tendency (Fig. 6). The lack of saturation reflects that moments can be flipped to the field direction only if the field is applied along the *c* or *b* direction. The magnetization values actually exceed those found for single crystal sample in the field-aligned state (1.45 μ_B/f.u.) [21]. UNiGe has no remanence and exhibits a hysteretic metamagnetic behavior in the range of 3–5 T. This corresponds to the magnetization curve presented for a fixed-powder sample in Ref. [22]. The critical metamagnetic fields shift to very high values for grains with the *a* direction close to the field direction. The magnetization of the UNiGe hydrides reveals μ_S and approaches the saturation faster

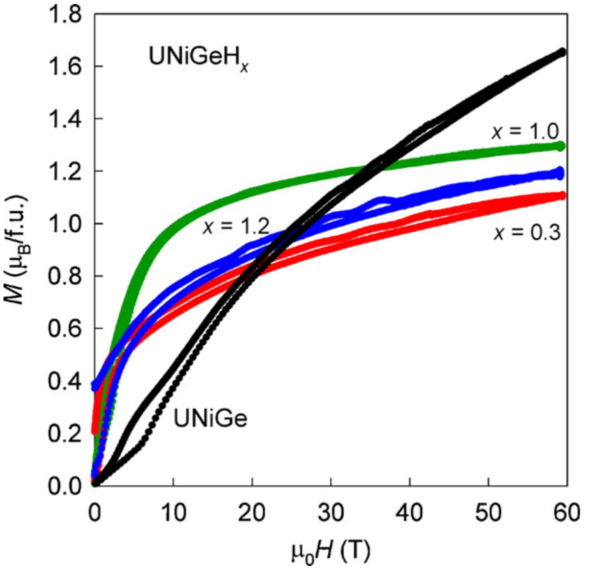

Fig. 6. Comparison of magnetization curves of UNiGeH$_x$ and UNiGe measured in pulsed magnetic field swept up and down up to 60 T at T = 1.5 K [14].

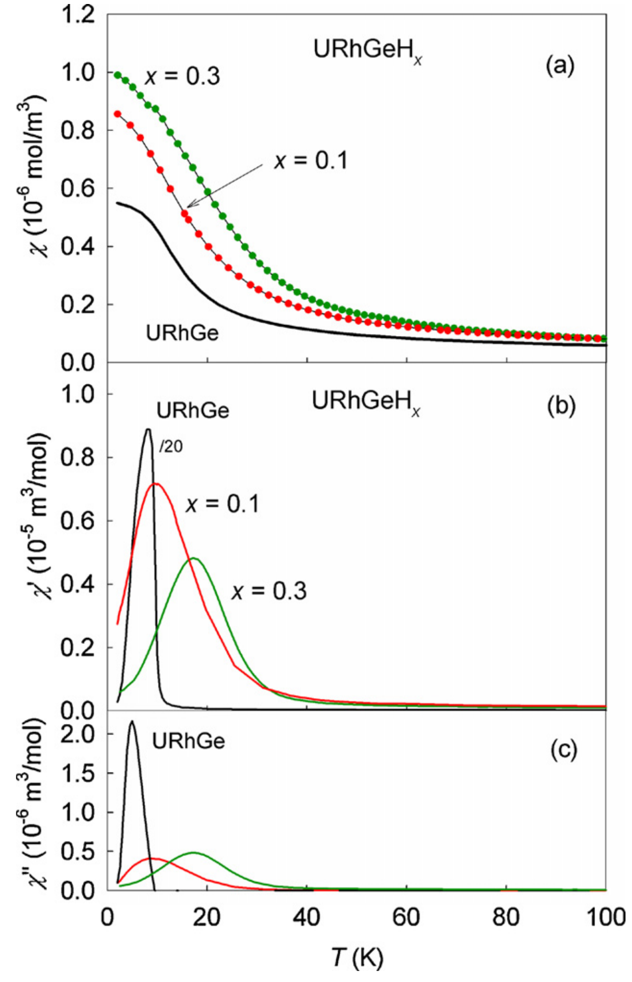

Fig. 7. (a) Temperature dependence of *dc* susceptibilities for URhGeH$_x$ and URhGe measured in μ_0H = 3 T. (b) Real and (c) imaginary part of *ac* susceptibilities for URhGeH$_x$ and URhGe measured in zero *dc* field and *ac* field of 1 mT and frequency 80 Hz.

(Fig. 6). As we saw for the fixed-powder data for UNiGe, metamagnetic transitions are not well resolved in this type of experiment on highly anisotropic materials. We can speculate that the relative fast increase in fields up to 10–12 T comprises actually metamagnetic transitions, which are displaced to lower fields compared to UNiGe. For more details see Ref. [14].

3.3. α-Hydrides of URhGe, UPdGe and UIrGe

URhGe is known to be a weak itinerant ferromagnet with T_C = 9.5 K [23]. Hydrogenation does not change the type of magnetic order in α-hydrides. Both of them remain F with enhanced T_C and their susceptibilities values (Fig. 7(a)). For URhGeH$_{0.1}$ a broad well-pronounced peak is observed in $\chi_{ac}(T)$ between 9 K and 20 K (Fig. 7(b) and (c)) [16]. The Arrott plots indicate that the sample is inhomogeneous, thus T_C could not be precisely determined for this hydride. In the case of URhGeH$_{0.3}$, the maximum seen in $\chi_{ac}(T)$ (Fig. 7(b) and (c)) is shifted towards higher temperatures. The Arrott plots indicate that the ordering temperature of URhGeH$_{0.3}$ is T_C = 17 K. Magnetization curves of α-hydrides measured at T = 2 K show a weak tendency to saturation at high magnetic fields of 9 T (Fig. 8). μ_S increases from 0.2 μ_B/f.u. for the parent compound up to 0.3 μ_B/f.u. and 0.38 μ_B/f.u. for the hydrides, for x = 0.1 and 0.3, respectively (Fig. 8).

The *dc* susceptibility measurements (Fig. 9(a)) for UPdGe and its α-hydride confirm the existence of the P-AF transition at about 50 K (T_N is not affected by hydrogenation) and the AF-F transition at 30 K for the pure compound [16] and 26 K for the hydride. The maxima seen in $\chi_{ac}(T)$ (Fig. 9(b) and (c)) point to the above mentioned transitions. The specific heat data for UPdGeH$_{0.1}$ display only a weak anomaly at T = 50 K. The magnetization curves measured at T = 2 K (Fig. 10(a)) approach saturation in high magnetic fields (≈9 T). μ_s (≈0.62 μ_B/f.u.) for UPdGeH$_{0.1}$ is higher than that for UPdGe ($\mu_s \approx$ 0.47 μ_B/f.u.). This can point to an enhanced stability of U magnetic moments.

$\chi_{dc}(T)$ and $\chi_{ac}(T)$ of UIrGe exhibit the AF transition around T_N = 17 K [23] (Fig. 11(a)–(c)). The type of magnetic order is changed in the α-hydride. The Arrott plots indicate T_C of 28 K for UIrGeH$_{0.1}$. Magnetization curve of UIrGeH$_{0.1}$ measured at T = 2 K exhibits a part of the broad hysteresis loop with μ_s of 0.3 μ_B/f.u. (Fig. 12). The metamagnetic transition reported for UIrGe at 14 T [24] is not

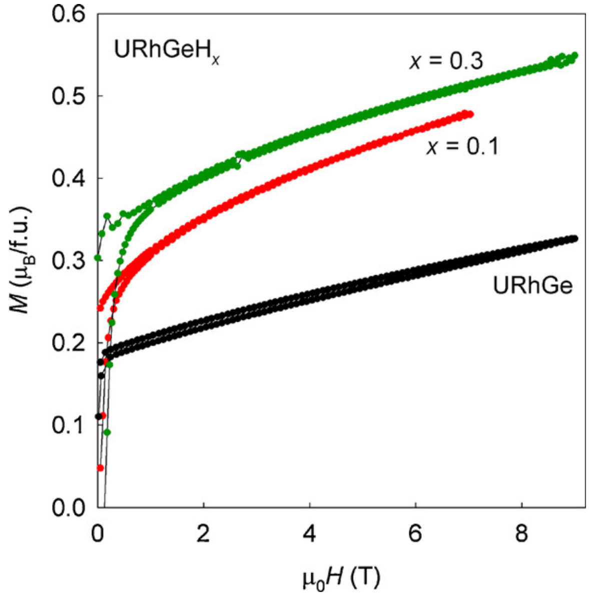

Fig. 8. Comparison of magnetization curves of URhGeH$_x$ and URhGe measured at T = 2 K.

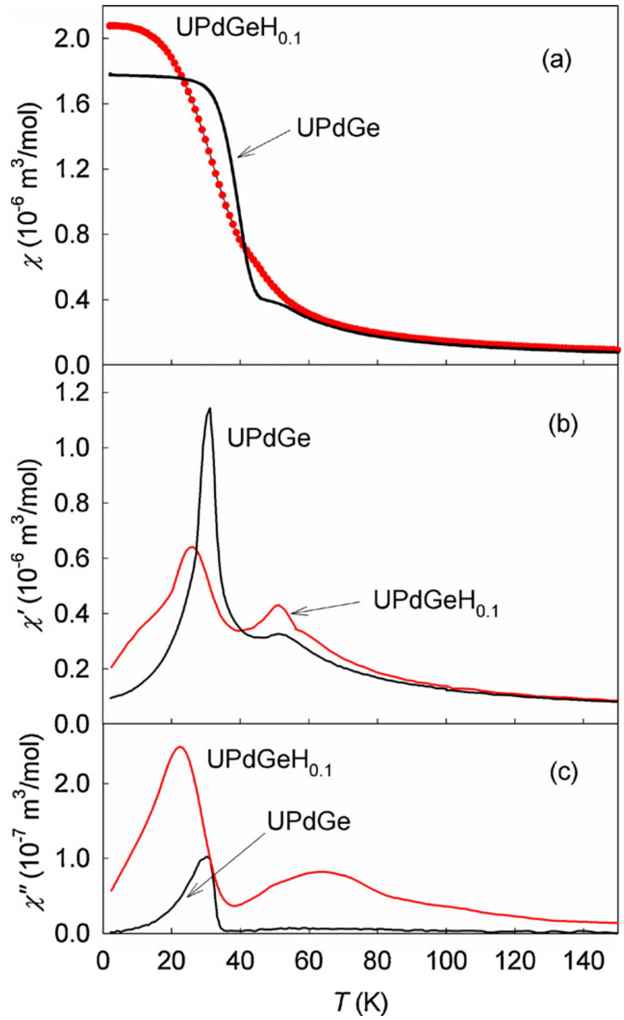

Fig. 9. (a) Temperature dependence of *dc* susceptibilities for UPdGe and its α-hydride measured in $\mu_0H = 2$ T. (b) Real and (c) imaginary part of *ac* susceptibilities for UPdGe and its α-hydride measured in zero *dc* field and *ac* field of 1 mT and frequency 80 Hz.

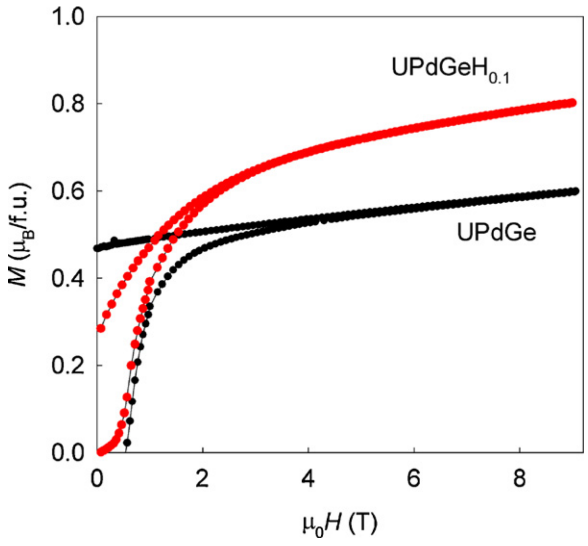

Fig. 10. Comparison of magnetization curves of UPdGe and its α-hydride measured at $T = 2$ K.

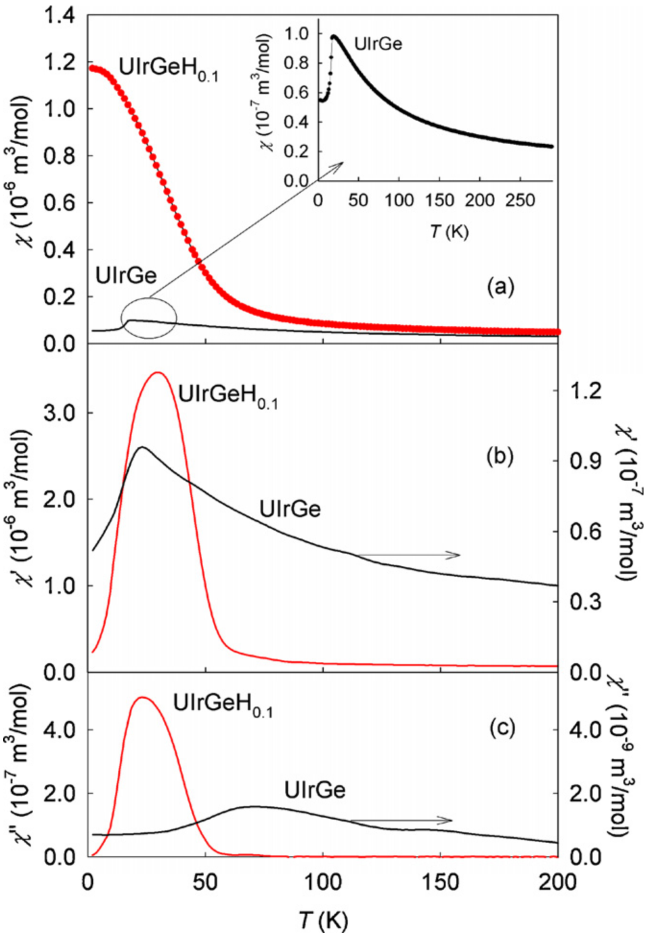

Fig. 11. (a) Temperature dependence of *dc* susceptibilities for UIrGe and its α-hydride measured in $\mu_0H = 2$ T. The inset shows the details of AF transition in UIrGe. (b) Real and (c) imaginary part of *ac* susceptibilities for UIrGe and its α-hydride measured in zero *dc* field and *ac* field of 1 mT and frequency 80 Hz.

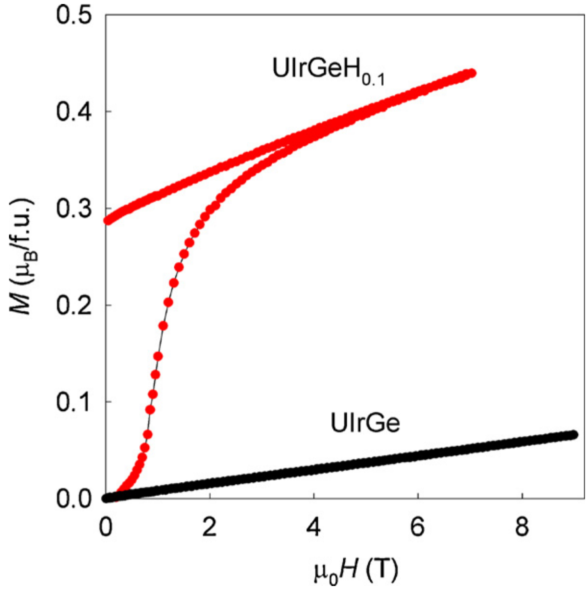

Fig. 12. Comparison of magnetization curves of UIrGe and its α-hydride measured at $T = 2$ K.

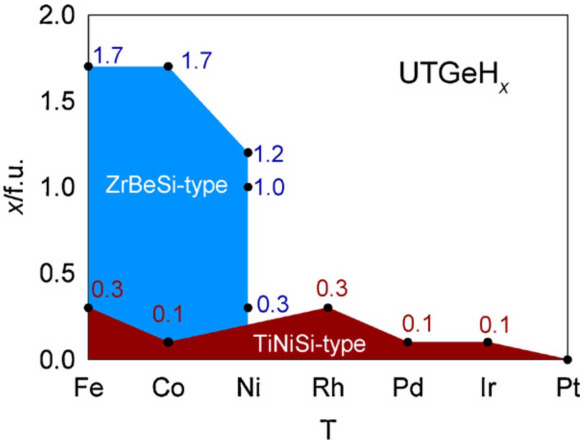

Fig. 13. Two types of UTGe hydrides and their H concentration.

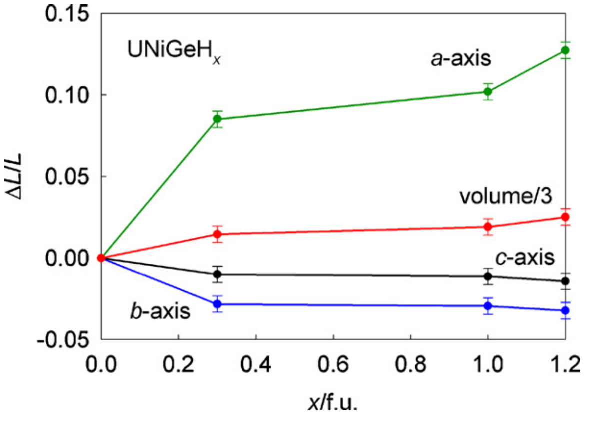

Fig. 14. Hydrogen variations of the relative changes of lattice parameters $\Delta a/a$, $\Delta b/b$, $\Delta c/c$ and volume $\Delta V/V$ for β-hydrides of UNiGe. The lattice parameters of hexagonal hydrides of UNiGe were recalculated for the orthorhombic representation.

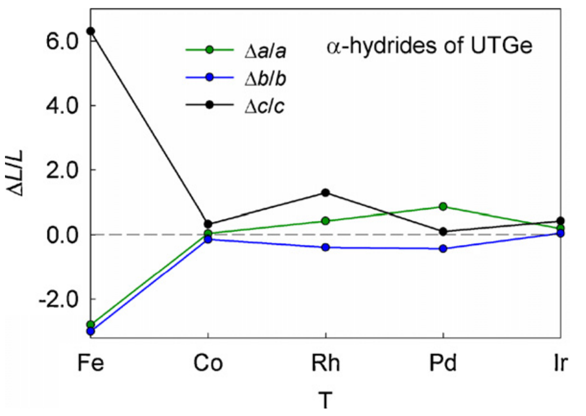

Fig. 15. The relative changes of the lattice parameters $\Delta a/a$, $\Delta b/b$, $\Delta c/c$ for α-hydrides of UTGe.

complete in Fig. 12, as the magnetization measurement was performed only up to 9 T.

4. Conclusions

Our detailed study of the UTGe hydrides underline the general tendency of strengthening of magnetic properties of U compounds due to hydrogenation. In this particular case, there is also a primary impact on the crystal structure. Due to the hydrogen absorption in UTGe, one can observe the transformation of the lattice from the orthorhombic TiNiSi-type (or its monoclinic variety) to the hexagonal ZrBeSi-type. Here it was documented for the compounds with the 3*d* transition metals (T = Fe, Co, Ni) as shown in Fig. 13. The volume expansion reaches the maximal value of 10.7% in $UCoGeH_{1.7}$ (obtained under $p_{H_2} = 2$ bar). The formation of β-hydrides is accompanied by a strongly anisotropic lattice expansion seen e.g. for UNiGe-H (Fig. 14). Using the orthorhombic representation, the crystal lattice of the β-hydrides expands along the *a* direction causing an increase of d_{U-U}. A contraction is observed along the *b*- and *c*-axis. The relative lattice expansion/compression e.g. in $UNiGeH_{1.2}$ ($\Delta a/a = 12.6\%$, $\Delta b/b = -3.4\%$, $\Delta c/c = -1.6\%$ and $\Delta V/V = 7.6\%$) can be compared with $LaNiSnD_2$ ($\Delta a/a = 12.9\%$, $\Delta b/b = -5.1\%$, $\Delta c/c = 0.7\%$ and $\Delta V/V = 7.9\%$ [10]). The only difference is observed along the *c* direction. For the compounds with the 4*d* and 5*d* transition metals (T = Rh, Pd and T = Ir), the structure type is not changed upon hydrogenation (Fig. 13). Hydrogenation leads only to a weak expansion of the unit cell about 0.5% and 1.3% for Pd and Rh, respectively. The crystal lattice of α-hydrides of UTGe compounds expands in two directions namely along the *a* or *c* direction and shrinks along the *b* direction (Fig. 15). One should notice that the anisotropy of lattice expansion is by far not equivalent to anisotropy of compressibility under hydrostatic pressure, observed so far for UCoGe [25].

The variations of magnetism upon hydrogenation can be dramatic. Hydrogen absorption can induce a change of the type of magnetic order, an additional phase transition, or a shift of the magnetic ordering temperature. These effects are displayed for UTGe-H

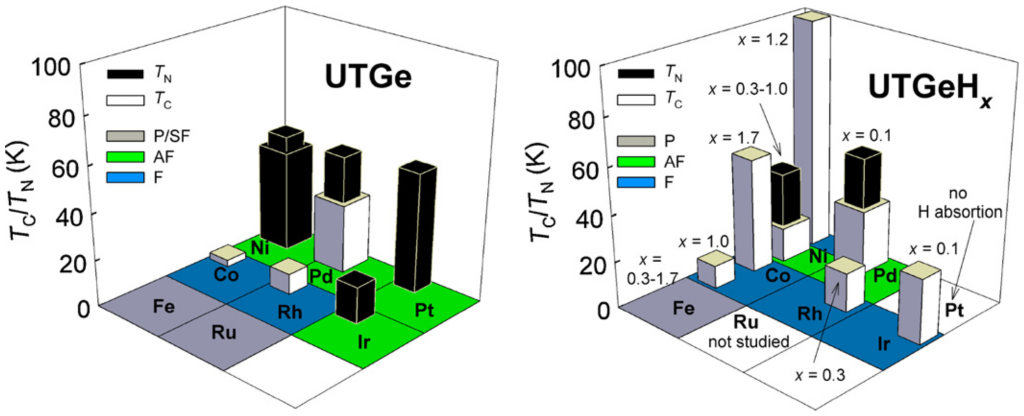

Fig. 16. Summary of magnetic properties of UTGe hydrides (right panel) compared with the parent UTGe compounds (left panel). The type of ground state of the initial compounds is indicated: P/SF – paramagnetic/spin fluctuator, AF – antiferromagnetic, F – ferromagnetic. The column-height shows the values of ordering temperatures (the white-colored column shows T_C and black one shows T_N).

compounds in Fig. 16. The AF turns into F one in UNiGeH$_{1.2}$ and UIrGeH$_{0.1}$. An additional phase transition appears in intermediate β-hydrides of UNiGe at 7–15 K and in two-β-phase hydrides of UCoGe at 8 K. A respective increase of T_C up to 50 K, and 17 K, was reported in the hydrides of two itinerant ferromagnets: UCoGe and URhGe. No significant changes upon hydrogenation are observed for UPdGe, despite of the volume expansion of 0.5%. UPtGe does not absorb detectable amount of hydrogen up to $p_{H_2} = 160$ bar and $T = 773$ K.

In general, observed changes in magnetism of UTGe compounds can be attributed to an enhancement of d_{U-U} and reducing the 5*f*–5*f* overlap. In the case of UFeGe, where the 5*f*-*d* hybridization is presumably strong, the hydrogen absorption can also lead to a reduction of the 5*f*-*d* hybridization, altogether implying an enhancement of magnetic interactions, but not on the level sufficient to induce any magnetic order. Our main conclusion is that the hydrogen absorption can be used as a convenient control parameter to tune magnetic properties of UTGe compounds.

Acknowledgements

This work was part of the research program MSM 0021620834. High-field magnetization measurements have been supported by EuroMagNET under the EU contract 228043.

References

[1] P. Raj, K. Shashikala, A. Sathyamoorthy, N. Harish Kumar, C.R. Venkateswara Rao, S.K. Malik, Phys. Rev. B 63 (2001) 094414.
[2] K. Miliyanchuk, L. Havela, A.V. Kolomiets, A.V. Andreev, J. Alloys Compd. 404–406 (2005) 165–168.
[3] L. Havela, K. Miliyanchuk, A.V. Kolomiets, L.C.J. Pereira, A.P. Gonçalves, E. Ŝantavá, K. Prokeš, J. Alloys Compd. 446–447 (2007) 606–609.
[4] K. Miliyanchuk, A.V. Kolomiets, L. Havela, A.V. Andreev, J. Alloys Compd. 383 (2004) 103–107.
[5] A.V. Kolomiets, L. Havela, A.V. Andreev, F. Wastin, J. Šebek, M. Maryško, Phys. Rev. B 66 (2002) 144423.
[6] F. Canepa, P. Manfrinetti, M. Pani, A. Palenzona, J. Alloys Compd. 234 (1996) 225.
[7] L. Havela, V. Sechovský, F.R. de Boer, E. Brück, H. Nakotte, Physica B 177 (1992) 159–163.
[8] Y. Skourski, M.D. Kuz'min, K.P. Skokov, A.V. Andreev, J. Wosnitza, Phys. Rev. B 83 (2011) 214420(9).
[9] H.W. Brinks, V.A. Yartys, B.C. Hauback, J. Alloys Compd. 322 (2001) 160.
[10] V.A. Yartys, T. Olavesen, B.C. Hauback, H. Fjellvåg, H.W. Brinks, J. Alloys Compd. 330–332 (2002) 141–145.
[11] K. Miliyanchuk, L. Havela, J.C. Waerenborgh, P. Gaczyński, O. Prokhnenko, Chem. Met. Alloys 1 (2008) 174–179.
[12] A.M. Adamska, L. Havela, A. Błachowski, K. Ruebenbauer, J.C. Waerenborgh, N.-T.H. Kim-Ngan, A.V. Kolomiets, J. Alloys Compd. 509 (2011) 5453–5459.
[13] A.M. Adamska, L. Havela, S. Daniš, J. Phys.: Condens. Matter 23 (2011) 476002.
[14] A.M. Adamska, L. Havela, J. Procházka, A.V. Andreev, Y. Skourski, J. Magn. Magn. Mater. 323 (2011) 3217–3222.
[15] A. Adamska, A. Kolomiets, J. Pospíšil, L. Havela, J. Phys.: Conf. Ser. 200 (2010) 012002.
[16] S. Kawamata, H. Iwasaki, N. Kobayashi, J. Magn. Magn. Mater. 104–107 (1992) 55–56.
[18] L. Havela, A. Kolomiets, V. Sechovsky, M. Diviš, M. Richter, A.V. Andreev, J. Magn. Magn. Mater. 177–181 (1998) 47.
[19] N.T. Huy, A. Gasparini, D.E. de Nijs, Y. Huang, J.C.P. Klaasse, T. Gortenmulder, A. de Visser, A. Hamann, T. Görlach, H. von Löhneysen, Phys. Rev. Lett. 99 (2007) 067006.
[20] A. Purwanto, V. Sechovsky, L. Havela, R.A. Robinson, H. Nakotte, A.C. Larson, K. Prokes, E. Brück, E.R. de Boer, Phys. Rev. B 53 (1996) 758.
[21] L. Havela, V. Sechovsky, R.F. de Boer, E. Brück, H. Nakotte, Physica B 177 (1992) 159–163.
[22] F.R. De Boer, E. Brück, V. Sechovsky, L. Havela, K.H.J. Buschow, Physica B 163 (1990) 175–178.
[23] R. Troć, V.H. Tran, J. Magn. Magn. Mater. 73 (1988) 389–397.
[24] S. Yoshii, A.V. Andreev, E. Brück, J.C.P. Klaasse, K. Prokeš, F.R. de Boer, M. Hagiwara, K. Kindo, V. Sechovský, J. Phys. Conf. Ser. 51 (2006) 151–154.
[25] A.M. Adamska, L. Havela, S. Surble, S. Heathman, J. Pospíšil, S. Daniš, J. Phys.: Condens. Matter 22 (2010) 275603.